Hierachy of Mesoscale Flow Assumptions and Equations

P. THUNIS

Environment Institute, Joint Research Center, Ispra, Italy, and Institut d'Astronomie de Geophysique, Louvain la Neuve, Belgium

R. BORNSTEIN

Environment Institute, Joint Research Center, Ispra, Italy, and Department of Meteorology, San Jose State University, San Jose, California

(Manuscript received 22 August 1994, in final form 3 August 1995)

ABSTRACT

The present research proposes a standard nomenclature for mesoscale meteorological concepts and integrates existing concepts of atmospheric space scales, flow assumptions, governing equations, and resulting motions into a hierarchy useful in categorization of mesoscale models. New dynamically based mesoscale time- and space-scale boundaries are proposed, consistent with the importance of the Coriolis force. In the proposed flow-class classification, the starting point is the complete (no approximations) set of mesoscale equations for non-Boussinesq flows. In the subsequent scale analysis, the deep and shallow Boussinesq flow divisions of Dutton and Fichtl are kept, as is the shallow-flow subdivisions of Mahrt. In addition, the scale analysis approach of Mahrt is extended to deep Boussinesq motions. Limits of applicability of each derived flow-class equation set (with respect to atmospheric phenomena that can be simulated) are also discussed.

The proposed hierarchy of atmospheric motions is organized into hydrostatic versus nonhydrostatic flow types and then into non-Boussinesq, deep, and shallow Boussinesq motions. Criteria used to differentiate each resulting flow class are discussed, while resulting governing thermodynamic and dynamic equations for each motion type are given. Separate graphical representations during stable and unstable conditions of the spatial limits of each Boussinesq mesoscale flow subclass are constructed from order of magnitude estimates for the various length and flow-class separation criteria. A summary of the consensus in the literature concerning the equation sets necessary to reproduce characteristics associated with specific atmospheric flow phenomena is given. Comparative modeling studies are required to test the quantitative aspects of many of the ideas put forth in this paper.

1. Introduction

Hasse (1993) recently called for a series of "perhaps controversial" papers to stimulate discussion on aspects toward development of a "commonly accepted planetary boundary layer (PBL) theory." Lack of agreement concerning technical definitions thwarts such a development. Previous examples in air pollution meteorology include diffusion versus dispersion and model validation versus evaluation.

Different opinions currently exist concerning definitions of the time and space boundaries of the micro-, meso-, and macrometeorological scales; Boussinesq approximations; anelastic equation of continuity; advection versus convection; and shallow convection. The present research begins with a review of the current status on these topics. It then proposes a standard nomenclature and integrates the concepts of atmospheric space scales, flow assumptions, governing equations, and resulting motions into a hierarchy useful for mesoscale model classification.

2. Atmospheric space scales

The standardization of mid-1970s atmospheric scale classification schemes by Orlanski (1975) contained eight horizontal space and time subdivisions (Table 1) because of the wide range of phenomena encompassed by the three basic scales (micro, meso, and macro). The previous definition of the mesoscale he quoted was intermediate states between macroscale ("space scales more that 1000 km and time scales of the order of a week") and microscale ("space scales of several meters and time scales on the order of a minute"). His proposed new upper bound (2000 km) was of the same order of magnitude as the old one, but his new lower bound (2 km) significantly enlarged the range of microscale phenomena. He pointed out, however, that as it was not generally possible to identify "a relationship between geophysical parameters and the intrinsic spatial scale, . . . all horizontal scale divisions are somewhat arbitrary and ill-defined."

Recent mesoscale texts, however, have proposed alternative definitions for mesoscale phenomena; for

Corresponding author address: Dr. Robert D. Bornstein, Department of Meteorology, San Jose State University, San Jose, CA 95192-0104.

TABLE 1. Atmospheric scale definitions, where L_H is horizontal scale length.

L_H	Lifetime	Stull (1988)	Pielke (1984)	Orlanski (1975)	Present	Atmospheric phenomena
10 000 km	1 month	Macro	Synoptic Regional	Macro-α	Macro-α	General circulation, long waves
2000 km	1 week			Macro-β	Macro-β	Synoptic cyclones
200 km	1 day		Meso	Meso-α	Macro-γ	Fronts, hurricanes
20 km	1 h	Meso		Meso-β	Meso-β	Low-level jets, thunderstorm groups, mountain winds and waves, sea breeze, urban circulations
2 km				Meso-γ	Meso-γ	Thunderstorm, clear-air turbulence
200 m	30 min	Micro	Micro	Micro-α	Meso-δ	Cumulus, tornadoes, katabatic jumps
20 m	1 min			Micro-β	Micro-β	Plumes, wakes, waterspouts, dust devils
2 m	1 s	Micro δ		Micro-γ	Micro-γ	Turbulence, sound waves
					Micro-δ	

example, the textbook of Arya (1988) defines micrometeorological phenomena as limited to those that "originate in and are dominated by" the PBL, excluding phenomena whose "dynamics are largely governed by mesoscale and macroscale weather systems." The textbook of Pielke (1984) defines mesoscale phenomena as having a horizontal length scale large enough to be hydrostatic but small enough so that the Coriolis force is small relative to the advective and pressure gradient forces. While Pielke mentions that this upper

bound is thus latitude dependent, it is also true that his lower bound would be PBL stability dependent. His definition (Table 1) thus confines mesoscale to the Orlanski meso-β scale.

The mesoscale bounds of Pielke were consistent with phenomena that contemporaneous mesomodels could simulate, that is, meso-β. Such models generally used meso-α (and larger) values as external forcing and parameterized subgrid/subscale nonhydrostatic (meso-γ and smaller) effects. Current nonhydrostatic mesoscale models are, however, capable of simulating motions on the smaller meso-γ and micro-α scales, while model nesting allows them to simulate meso-α (and larger) flows.

The textbook of Stull (1988) places the lower limit of the mesoscale at 3 km. It also reproduces part of the Orlanski table (meso-α to micro-γ) but with an additional micro-δ scale (Table 1) extending from 2 m down to 2 mm. In addition, it shows an overlap between the micro- and mesoscales that extends downward from the middle of meso-γ to the lower end of micro-α.

Pielke (1984) also defines the vertical bounds of mesoscale phenomena as extending "from tens of meters (i.e., above the SBL) to the depth of the troposphere." While shallow mesoscale motions (like sea breezes) are all or mostly contained within the PBL, deep mesoscale motions (like thunderstorms) can extend well above it.

Given the current variety of definitions for both mesoscale bounds, the current work seeks to update the Orlanski subdivisions. The new proposed scale boundaries (Table 1) include the following changes: addition of a micro-δ scale, renaming of meso α to macro γ, and renaming of micro α to meso δ. These last two changes shift mesoscale down one class toward smaller-scale flows. These changes thus incorporate contributions from the boundary layer meteorology textbook of Stull, except that his scheme showed an overlap of the micro- and mesoscales covering the current meso δ and half of the current meso γ.

Both new mesoscale boundaries (appendix A) are thus dynamically based. Its upper boundary thus corresponds to that proposed by the textbook of Pielke, in which atmospheric motions have a horizontal extent small enough so that the Coriolis force is not latitude dependant. By analogy, the new lower bound includes all phenomena in which Coriolis effects are strong enough to determine rotational direction. Note that both new mesoscale bounds are stability dependent, because as stability increases, motions become more horizontal and thus more influenced by Coriolis forcing.

Dust devils and water spouts are thus microscale, as they are in cyclostrophic balance and can rotate in either direction (Table 1). While tornadoes are also cyclostrophic, they are large enough so that Coriolis forcing generally determines flow direction (but not speed), hence, they are mesoscale. While the current upper limit excludes phenomena in which latitude-dependent effects are significant (such as fronts and hurricanes), it does include tropospheric phenomena either originating at the surface or driven by dynamic macroscale weather systems, for example, squall-line thunderstorms.

The location in Table 1 of only two phenomena differ from that in Orlanski and Stull; that is, plumes and urban effects are each moved up one scale. Current mesomodels can simulate flows on all proposed meso subscales, including nonhydrostatic meso-γ and meso-δ phenomena, as discussed below.

3. Governing equations

The different flow depths of the various mesoscale flow types imply governing dynamic and thermodynamic equations that can be simplified via scaling assumptions such as the Boussinesq approximation. Disagreement exists, however, as to the vertical extent to which that approximation is valid. A description of the approximations of Boussinesq (1903) always states that the variation of perturbation density can be neglected in the mass continuity and momentum equations, except through its influence in the buoyancy term (which includes thermal and pressure contributions) in the vertical equation of motion (appendix A). Such a statement allows for both deep and shallow flows (Dutton and Fichtl 1969; Pielke 1984). Some authors (e.g., Businger 1982), however, further impose a condition that perturbation pressure influences in the buoyancy term can be neglected, which restricts the approximation to shallow flows. Mahrt (1986) and Stull (1988) point out that this extra condition is limited to only nonneutral shallow flows.

The current study attempts to clarify the types of Boussinesq and non-Boussinesq atmospheric flows and to identify the approximations implied in the derivation of their respective governing equations. The current research keeps the deep and shallow Boussinesq flow equations of Dutton and Fichtl and the shallow flow subdivisions of Mahrt. In addition, the scale analysis approach of Mahrt is extended to deep motions. Limits of applicability of each equation set (with respect to atmospheric phenomena that can be simulated) are also discussed.

In engineering terminology, convection is used to describe vertical or horizontal movements of mass or energy by either the mean or turbulent component of thermally forced flow. In meteorology, convection needs to be differentiated from both advection and diffusion (appendix A). The smallest scale of the vertical movement of energy, mass, and/or momentum is random (disorganized) microscale turbulent diffusion (with a zero-mean vertical velocity). The next largest scale of such movement is organized (nonhydrostatic) mesoscale or microscale (thermal or mechanical) convection, with vertical velocities large enough (same order of magnitude as horizontal velocities) to signifi-

cantly alter or produce the horizontal flow component (mainly) by mass continuity. Finally, the largest scale of vertical movement is the organized mesoscale (and larger) advective circulation cells, in which advective vertical velocities are at least an order smaller than the horizontal component and arise from horizontal convergence again via mass continuity.

One impact of such a nomenclature is that motions such as sea–land breezes, mountain–valley winds, and urban circulations would no longer be referred to as convective but as advective. Another result of this classification is also that hydrostatic mountain waves are considered as advective, while nonlinear lee waves are convective. Note, this does not imply that all nonhydrostatic flows are convective, that is, neutral-stability advective flows over surface discontinuities in which vertical motions are limited by advection are also nonhydrostatic (Fig. 1). All hydrostatic flows are thus advective, but not all advective flows are hydrostatic.

a. Basic equations

The instantaneous $(\tilde{\ })$ momentum and continuity equations are, respectively,

$$\tilde{\rho}\frac{\partial \tilde{\mathbf{V}}}{\partial t} = -\tilde{\rho}\tilde{\mathbf{V}}\cdot\nabla\tilde{\mathbf{V}} - \nabla\tilde{p} - \tilde{\rho}g\delta_{i3} - 2\tilde{\rho}\boldsymbol{\Omega}\times\tilde{\mathbf{V}} + \mu\nabla^2\tilde{\mathbf{V}}, \quad (1)$$

$$\frac{\partial \tilde{\rho}}{\partial t} = -\nabla\cdot\tilde{\rho}\tilde{\mathbf{V}}, \quad (2)$$

where all symbols are defined in appendix B. Combining both equations yields

$$\frac{\partial \tilde{\rho}\tilde{\mathbf{V}}}{\partial t} = -\nabla\cdot\tilde{\rho}\tilde{\mathbf{V}}\tilde{\mathbf{V}} - \nabla\tilde{p} - \tilde{\rho}g\delta_{i3} - 2\tilde{\rho}\boldsymbol{\Omega}\times\tilde{\mathbf{V}} + \mu\nabla^2\tilde{\mathbf{V}}. \quad (3)$$

Each thermodynamic and dynamic parameter in the above two equations is then Reynolds decomposed (appendix A) into its mean (unbarred for convenience) and turbulent components:

$$(\tilde{\ }) = (\ ) + (\ )',$$

in which

$$(\ ) = \frac{\int_t^{t+\Delta t}\int_x^{x+\Delta x}\int_y^{y+\Delta y}\int_z^{z+\Delta z}(\tilde{\ })\,dxdydzdt}{\Delta x\Delta y\Delta z\Delta t} \quad (4)$$

represents a running mean (appendix A). The Reynolds (averaging) assumption (appendix A) is then applied to the Reynolds decomposed versions of (2) and (3) to produce

$$\frac{\partial \rho}{\partial t} = -\nabla\cdot\rho\mathbf{V} - \nabla\cdot\overline{\rho'\mathbf{V}'}, \quad (5)$$

$$\frac{\partial \rho\mathbf{V}}{\partial t} = -\nabla\cdot(\rho\mathbf{V}\mathbf{V}) - \nabla\cdot(\rho\overline{\mathbf{V}'\mathbf{V}'}) + \mathbf{Mt} - \nabla p - \rho g\delta_{i3} - 2\rho\boldsymbol{\Omega}\times\mathbf{V} + \mu\nabla^2\mathbf{V}, \quad (6)$$

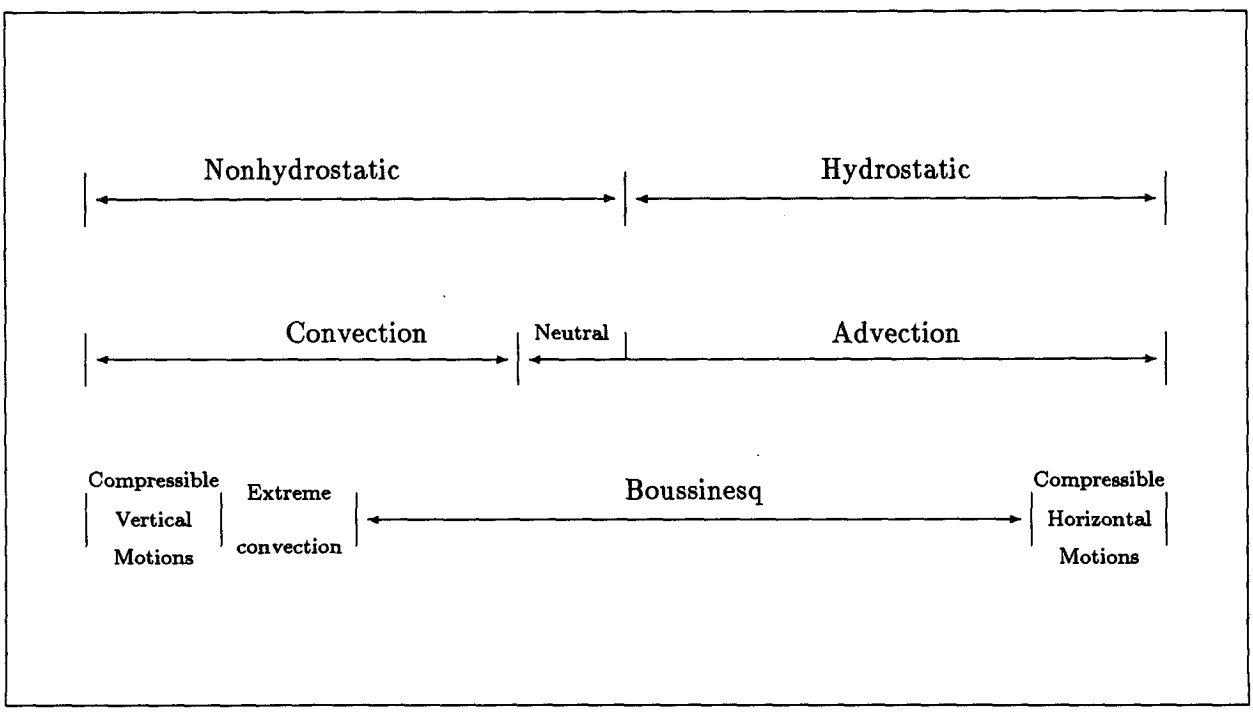

FIG. 1. Schematic of basic flow subclasses and assumptions.

where flux terms have an overbar and where the vector momentum turbulence term **Mt** is given by

$$\mathbf{Mt} = -\left(\frac{\partial(\overline{\rho'\mathbf{V}'})}{\partial t} + \nabla\cdot(2\mathbf{V}\overline{\rho'\mathbf{V}'} + \overline{\rho'\mathbf{V}'\mathbf{V}'}) + 2\boldsymbol{\Omega}\times\overline{\rho'\mathbf{V}'}\right).$$

Note, **Mt** contains density–velocity turbulent terms but no pressure–density perturbation term, as the starting equation (1) was multiplied by ρ to combine it with (2) to produce an equation containing diffusion terms.

Note, the validity of the Reynolds assumption requires the existence of a spectral gap scale separation between resolvable motions and parameterized subgrid processes (Pielke 1984). As recent observations show that such a separation generally does not exist (Young 1987; Courtney and Troen 1990), this assumption is questionable and should be applied carefully.

Also, the assumption (made in the above derivation) that spatiotemporal averages of time or space derivatives are equal to time or space derivatives of spatiotemporal averages is only valid in models with constant time steps of integration and/or constant grid spacings (Pielke 1984); for example,

$$\frac{(\partial\ )}{\partial t} = \frac{\partial(\ \ )}{\partial t}.$$

b. Timescaling

As only the vertical momentum and continuity equations are significantly modified in the following flow-class analysis, their most general forms [(5) and (6)] are given in the upper line of Table 2. Following Mahrt, the Coriolis and molecular viscosity terms are omitted in the table and in the following scale analysis, as their form would not be significantly altered. The same criterion is used to omit turbulent diffusion terms but to include the other turbulence terms in **Mt**.

Continuity equation (5), without its turbulence term, is now simplified via scale analysis, starting with decomposition (following Oberbeck 1888) of mean dynamic and thermodynamic variables $\phi(x, y, z, t)$ into a motionless (hydrostatic) horizontally homogeneous basic-state part $\phi_0(z)$ and a space/time-varying perturbation part $\phi_{hn}(x, y, z, t)$ that is the sum of hydrostatic $\phi_h(x, y, z, t)$ and nonhydrostatic $\phi_n(x, y, z, t)$ components.

This allows the compressible form of the mass continuity equation to be written as

$$\frac{\partial\alpha_{hn}}{\partial t} + \mathbf{V}_H\cdot\nabla_H\alpha_{hn} + w\frac{\partial\alpha_{hn}}{\partial z} + w\frac{\partial\alpha_0}{\partial z} = \alpha_0\nabla_H\cdot\mathbf{V}_H + \alpha_0\frac{\partial w}{\partial z}. \quad (7)$$

Typical mesoscale $(\ )_M$ and static-state $(\ )_s$ scale lengths, speeds, and times can be substituted in the above equation. In the current analysis, specific numerical values are not assigned to scale parameters, as these values are application dependent. After such substitution, (7) can be written as

$$\frac{\alpha_M}{\tau} + V_H\frac{\alpha_M}{L_H} + W\frac{\alpha_M}{L_z} + W\frac{\alpha_s}{H_\alpha} = \alpha_s\frac{V_H}{L_H} + \alpha_s\frac{W}{L_z}, \quad (8)$$

or

$$\frac{1}{\tau} + \frac{V_H}{L_H} + \frac{W}{L_z} + \frac{\alpha_s}{\alpha_M}\frac{W}{H_\alpha} = \frac{\alpha_s}{\alpha_M}\frac{V_H}{L_H} + \frac{\alpha_s}{\alpha_M}\frac{W}{L_z}, \quad (9)$$

where static-state density scale-height H_α is given by

$$H_\alpha = \left|\frac{1}{\alpha_s}\frac{\partial\alpha_s}{\partial z}\right|^{-1}.$$

Scale analysis identifies an appropriate timescale τ for the occurrence of significant variations in mesoscale specific volume. When τ is exceeded, the Eulerian time derivative of the mesoscale perturbation density can be neglected. Mahrt has summarized past approaches for obtaining τ.

Spiegel and Veronis (1960) and Businger (1982) assumed horizontal and vertical velocity advection scales of the same magnitude as the Eulerian time derivative of density; that is,

$$\tau \approx \frac{L_H}{V_H} \approx \frac{L_z}{W}. \quad (10)$$

When (10) is used in (9), the following is obtained

$$1 + 1 + 1 + \frac{\alpha_s}{\alpha_M}\frac{L_z}{H_\alpha} = \frac{\alpha_s}{\alpha_M} + \frac{\alpha_s}{\alpha_M}. \quad (11)$$

As they also assumed

$$\frac{|\alpha_M|}{|\alpha_s|} \ll 1, \quad (12)$$

the first three terms of (11) are neglected compared to the final two terms.

As they also only considered shallow flows,

$$L_z \ll H_\alpha, \quad (13)$$

the fourth term of (11) is also neglected, leaving only the nondivergent/incompressible form of the continuity equation (appendix A):

$$\nabla\cdot\mathbf{V} = 0. \quad (14)$$

Note that for flows over terrain features, L_z is the flow depth in the vertical (and not in the direction perpendicular to the surface).

According to Mahrt, however, use of (10) to derive (14) is invalid for flows when τ is either smaller or bigger than the advective timescales. In the former, density advection is dominated by mass convergence, which can be either due to the propagation of energy by pressure fluctuations or to density changes from ra-

TABLE 2. Governing equations for proposed flow subclass, where all symbols are defined in appendix B.

Flow sub-class		Partial Vert. Eq. of Motion	Thermal Energy Eq.	Continuity Eq.
Non Bouss. Motions	Comp.	$\frac{1}{\rho}\frac{\partial \rho w}{\partial t} = -\frac{1}{\rho}\nabla\cdot(\rho V w) - \frac{1}{\rho}\frac{\partial p_{hn}}{\partial z} - \frac{\rho_{hn}}{\rho}g + Mt$	$\frac{\partial \theta_{hn}}{\partial t} = -V\cdot\nabla\theta + \frac{\theta}{T}\left[\frac{\partial T_{hn}}{\partial t} - \frac{\alpha}{c_p}\frac{\partial p_{hn}}{\partial t}\right]_D + Et$	$-\frac{\partial \rho_{hn}}{\partial t} = \nabla\cdot(V\rho) + \nabla\cdot(\overline{V'\rho'})$
	Motions Horiz.	$0 = -\frac{1}{\rho}\frac{\partial p_h}{\partial z} - \frac{\rho_h}{\rho}g$		
Motions	Extreme Convect.	$\frac{\partial w}{\partial t} = -\frac{1}{\rho}\nabla\cdot(\rho V w) - \frac{1}{\rho}\frac{\partial p_{hn}}{\partial z} - \frac{\rho_{hn}}{\rho}g + Mt$	$\frac{\partial \theta_{hn}}{\partial t} = -\frac{1}{\tilde{\rho}}\nabla\cdot(\tilde{\rho}V\theta) + \frac{\theta}{T}\left[\frac{\partial T_{hn}}{\partial t} - \frac{\alpha}{c_p}\frac{\partial p_{hn}}{\partial t}\right]_D + Et$	$0 = \nabla\cdot(V\rho) + \nabla\cdot(\overline{V'\rho'})$
Deep Bouss. Motions	Deep Convect.	$\frac{\partial w}{\partial t} = -\frac{1}{\rho_o}\nabla\cdot(\rho_o V w) - \frac{1}{\rho_o}\frac{\partial p_{hn}}{\partial z} + g\left(\frac{\theta_{hn}}{\theta_o} - \frac{c_v}{c_p}\frac{p_{hn}}{p_o}\right)$	$\frac{\partial \theta_{hn}}{\partial t} = -\frac{1}{\rho_o}\nabla\cdot(\rho_o V\theta_{hn}) - w\frac{\partial \theta_o}{\partial z} + \frac{\theta_o}{T_o}\left[\frac{\partial T_{hn}}{\partial t} - \frac{\alpha_o}{c_p}\frac{\partial p_{hn}}{\partial t}\right]_D$	$0 = \nabla\cdot(V\rho_o)$
	Therm-D Advect.	$0 = -\frac{1}{\rho_o}\frac{\partial p_h}{\partial z} + g\left(\frac{\theta_h}{\theta_o} - \frac{c_v}{c_p}\frac{p_h}{p_o}\right)$		
Motions	Thermal Convect.	$\frac{\partial w}{\partial t} = -\frac{1}{\rho_o}\nabla\cdot(\rho_o V w) - \frac{1}{\rho_o}\frac{\partial p_{hn}}{\partial z} + g\frac{\theta_{hn}}{\theta_o}$	$\frac{\partial \theta_{hn}}{\partial t} = -\frac{1}{\rho_o}\nabla\cdot(\rho_o V\theta_{hn}) - w\frac{\partial \theta_o}{\partial z} + \frac{\theta_o}{T_o}\left[\frac{\partial T_{hn}}{\partial t}\right]_D$	
Shallow Bouss. Motions	Shallow Convect.	$\frac{\partial w}{\partial t} = -\nabla\cdot(Vw) - \frac{1}{\rho_a}\frac{\partial p_{hn}}{\partial z} + g\left(\frac{\theta_{hn}}{\theta_o} - \frac{c_v}{c_p}\frac{p_{hn}}{p_o}\right)$	$\frac{\partial \theta_{hn}}{\partial t} = -\nabla\cdot(V\theta_{hn}) - w\frac{\partial \theta_o}{\partial z} + \frac{\theta_o}{T_o}\left[\frac{\partial T_{hn}}{\partial t} - \frac{\alpha_a}{c_p}\frac{\partial p_{hn}}{\partial t}\right]_D$	$0 = \nabla\cdot V$
	Neutral Advect.	$\frac{\partial w}{\partial t} = -\nabla\cdot(Vw) - \frac{1}{\rho_a}\frac{\partial p_{hn}}{\partial z} - g\left(\frac{c_v}{c_p}\frac{p_{hn}}{p_o}\right)$		
	Thermal Advect.	$0 = -\frac{1}{\rho_a}\frac{\partial p_h}{\partial z} + g\frac{\theta_h}{\theta_o}$	$\frac{\partial \theta_{hn}}{\partial t} = -\nabla\cdot(V\theta_{hn}) - w\frac{\partial \theta_o}{\partial z} + \frac{\theta_o}{T_o}\left[\frac{\partial T_{hn}}{\partial t} - \frac{\alpha_a}{c_p}\frac{\partial p_{hn}}{\partial t}\right]_D$	
Motions	Thermal Convect.	$\frac{\partial w}{\partial t} = -\nabla\cdot(Vw) - \frac{1}{\rho_a}\frac{\partial p_{hn}}{\partial z} + g\frac{\theta_{hn}}{\theta_o}$		

diative flux divergence and/or phase changes. Thus, in theory, the Eulerian time derivative would be kept for such flows; however, as shown below, a less stringent criteria may be derived from τ that would in fact allow most such flows (sound waves excepted) to be governed by (14). In the opposite case, when τ is larger than the advective timescale (as in stationary conditions), the Eulerian derivative cannot be dropped, but the density perturbation advection terms can be dropped via (12).

As Ogura and Phillips (1962) and Dutton and Fichtl (1969) investigated convective flows, they assumed τ comparable to the buoyancy (Brunt–Väisälä) timescale, or

$$\tau \sim \frac{W}{g}\frac{\alpha_s}{\alpha_M}. \tag{15}$$

To neglect the Eulerian time derivative, their scale analysis showed it is necessary that

$$\tau \gg \sqrt{L_z/g}. \tag{16}$$

Note that Mahrt (1986) omitted the radical sign in his restatement of the above relationship. Advection of perturbation density is, however, only eliminated when

$$\frac{V_H}{W} \ll \frac{L_H}{L_z}. \tag{17}$$

The continuity equation thus again becomes the incompressible form given by (14) for shallow flows [in which (13) is valid] but becomes

$$\nabla\cdot\rho_0\mathbf{V} = 0 \tag{18}$$

for deep flows in which

$$L_z \ll H_\alpha. \tag{19}$$

While (18) is referred to as the anelastic form of the continuity equation, this name is also used for (derived below)

$$\nabla\cdot\rho\mathbf{V} = 0, \tag{20}$$

in which total density replaces ρ_0. Thus, (18) will hereafter be referred to as the Boussinesq anelastic form (appendix A), while (20) will be called the full anelastic form. As pointed out by Mahrt, (15) is not valid for near-neutral flows.

To correct the aforementioned limitations of Spiegel and Veronis and of Dutton and Fichtl, Mahrt derived a condition for τ by comparison of the Eulerian time derivative of density with the larger of the two velocity divergence terms on the right-hand side of (8), thus obtaining (after inversion of the terms)

$$\tau \gg \frac{\alpha_M}{\alpha_s}\left[\frac{L_H}{V_H}, \frac{L_z}{W}\right]_{\min}. \tag{21}$$

Note, this approach assumes that the perturbation density advection terms are dropped because of (12) and that the vertical static-state density advection term is dropped because of (13), which means that only shallow flows are considered. Equation (21) is a "partial" relaxation of the criteria of the preceding four studies, in that it allows for inclusion of most shallow flow types excluded by (10) and (15). It, however, excludes non-Boussinesq flows but does incorporate the deep Boussinesq flows of Dutton and Fichtl. A more relaxed condition on τ is now thus derived.

c. *Non-Boussinesq flows*

Whereas each of the above studies chose to compare the Eulerian derivative of the full (compressible) form of the continuity equation to only some of the other terms in the equation, the current extension of Mahrt's approach compares it to the largest of all the other five terms, yielding

$$\frac{\alpha_M}{\tau} \ll \left[V_H\frac{\alpha_M}{L_H}, W\frac{\alpha_M}{L_z}, W\frac{\alpha_s}{H_\alpha}, \alpha_s\frac{V_H}{L_H}, \alpha_s\frac{W}{L_z}\right]_{\max} \tag{22}$$

or

$$\tau \gg \left[\frac{L_H}{V_H}, \frac{L_z}{W}, \frac{\alpha_M}{\alpha_s}\frac{H_\alpha}{W}, \frac{\alpha_M}{\alpha_s}\frac{L_H}{V_H}, \frac{\alpha_M}{\alpha_s}\frac{L_z}{W}\right]_{\min}. \tag{23}$$

The new criteria is a relaxation of (21), as it now includes three new terms (final three) that might be smaller than the first two for flows either deeper than H_α (last versus third term) or in which

$$|\alpha_M| \geq |\alpha_s| \tag{24}$$

(fourth and fifth versus first and second terms). If, as is likely, (24) never occurs in normal atmospheric flows, (23) reduces to

$$\tau \gg \frac{\alpha_M}{\alpha_s}\left[\frac{L_H}{V_H}, \frac{L_z}{W}, \frac{H_\alpha}{W}\right]_{\min}. \tag{25}$$

Thus, flows with small τ values, that is, those not fulfilling (25), require the compressible form (appendix A) of the mass continuity equation (5) in Table 2 and are referred to as *compressible motions* (appendix A). Note, specific volume α appears in the text, but Table 2 equations are written in terms of density ρ for convenience.

Neglect of the turbulent density term in the continuity equation (and also in the momentum equation) has been shown by Mahrt (1986) as an invalid approximation in extreme aspect ratio flows, that is, extreme narrow convective and long thin horizontal advective flows.

While the flow speeds associated with normal meteorological phenomena are insufficient to alter atmospheric density, the complete continuity equation is kept in some models to avoid the necessity of solving

an elliptic equation for pressure. Solution of the compressible continuity equation, however, requires a small computational time step (as it allows for formation and propagation of sound waves, which are not of meteorological interest). It has thus been used for numerical convenience in GCMs, cloud models, and some mesoscale models (listed below).

Compressible motions can be nonhydrostatic or hydrostatic (Table 2 and appendix A). Nonhydrostatic compressible motions include vertical sound waves, while hydrostatic compressible motions include horizontal sound (or Lamb) waves (Table 3).

Compressible motions require the complete forms of the momentum and continuity equations, which are also valid for all Table 2 flow types (discussed below) derived by their simplification. Likewise, each set of equations in the table is also thus valid for flow types located below it, as indicated by the downward- and leftward-directed arrows in Fig. 2. The name in each box in the figure represents the most complex flow type reproducible with its associated equations (Table 2) but which cannot be simulated with equations associated with boxes located below it. Horizontal box position (solid-line part) is likewise related to the division between hydrostatic and nonhydrostatic motions, while dashed extensions into the hydrostatic part of the figure indicate that its equations are also able to simulate hydrostatic phenomena. Note that vertical location in Fig. 2 is not indicative of circulation depth, for example, as compressible motion sound waves can occur in shallow near-surface layers.

Nonhydrostatic (vertical) compressible motion models (Table 3) include MESOSCOP (Schumann et al. 1987), ADREA (Bartzis et al. 1991), and MM5 (Dudhia 1993), while hydrostatic (horizontal) formulations include MAR (Gallée and Schayes 1994) and MM4 (Anthes et al. 1987). Some models are quasi-nonhydrostatic, in that they do not include nonhydrostatic effects in all terms; for example, the buoyancy term in MEMO (Moussiopoulos et al. 1993) includes only hydrostatic density.

For larger τ values fulfilling (25), the Eulerian density time derivative can be dropped, and thus such flows require only the full anelastic mass continuity equation (20) in Table 2. Note that the turbulent density terms are still retained, as these flows are not limited in vertical extent. Hence, they are called *extreme convection* (appendix A) and, thus, are nonhydrostatic. Extreme convection flow types include nonlinear lee waves and severe thunderstorms (Table 3), but the authors have been unable to find any extreme convection models in the open literature. Note that none of the models listed under the two non-Boussinesq flow types in Table 3 are fully non-Boussinesq, as all omit the **Mt**, *Et*, and density velocity turbulent correlation terms.

d. Deep Boussinesq flows

Following Mahrt (1986), α' was kept in the non-Boussinesq flow equations discussed in the previous section. It is thus now proposed that the first criterion for Boussinesq motions is

$$|\alpha'| \ll |\alpha_s|, \tag{26}$$

which will be used as justification (in the averaged equations) to drop flux terms containing α'. This assumption was used by Pielke (1984) to eliminate the "turbulent density–pressure gradient correlation" term in the vertical equation of motion.

As described above, considerable work has been devoted to establishment of sufficient conditions for Boussinesq approximation validity. The above scale

TABLE 3. Examples of models used to simulate phenomena in text subclasses.

Subclass	Phenomena	Models	References
Compressible vertical motions	vertical sound waves	MESOSCOP	Schumann et al. (1987)
		MM5	Dudhia (1993)
		MEMO	Moussiopoulos et al. (1993)
		ADREA	Bartzis et al. (1991)
Compressible horizontal motions	horizontal sound waves	MAR	Gallée and Schayes (1994)
		MM4	Anthes et al. (1987)
Extreme convection	nonlinear lee waves, severe thunderstorms	—	—
Deep convection	thunderstorms, linear lee waves, orographic clouds	GESIMA	Eppel et al. (1992)
		RAMS	Tripoli and Cotton (1982)
		—	Peltier and Clark (1979)
Deep thermal convection	cumulus congestus	FITNAH	Gross (1992)
		TVMnh	Thunis (1995)
Thermodynamic advection	mountain waves, fronts, cyclones	—	—
Shallow convection	sea-breeze fronts	MERCURE	Buty et al. (1988)
Shallow thermal convection	cumulus, thermals, strong upslope winds	—	Sievers and Zdunkowski (1986)
		—	Svoboda and Stekl (1994)
Thermal advection	sea breezes, urban flows, mountain/valley winds down/upslope winds	URBMET/TVM	—
			Schayes et al. (1995)
Neutral advection	high wind speeds, low hill flows		

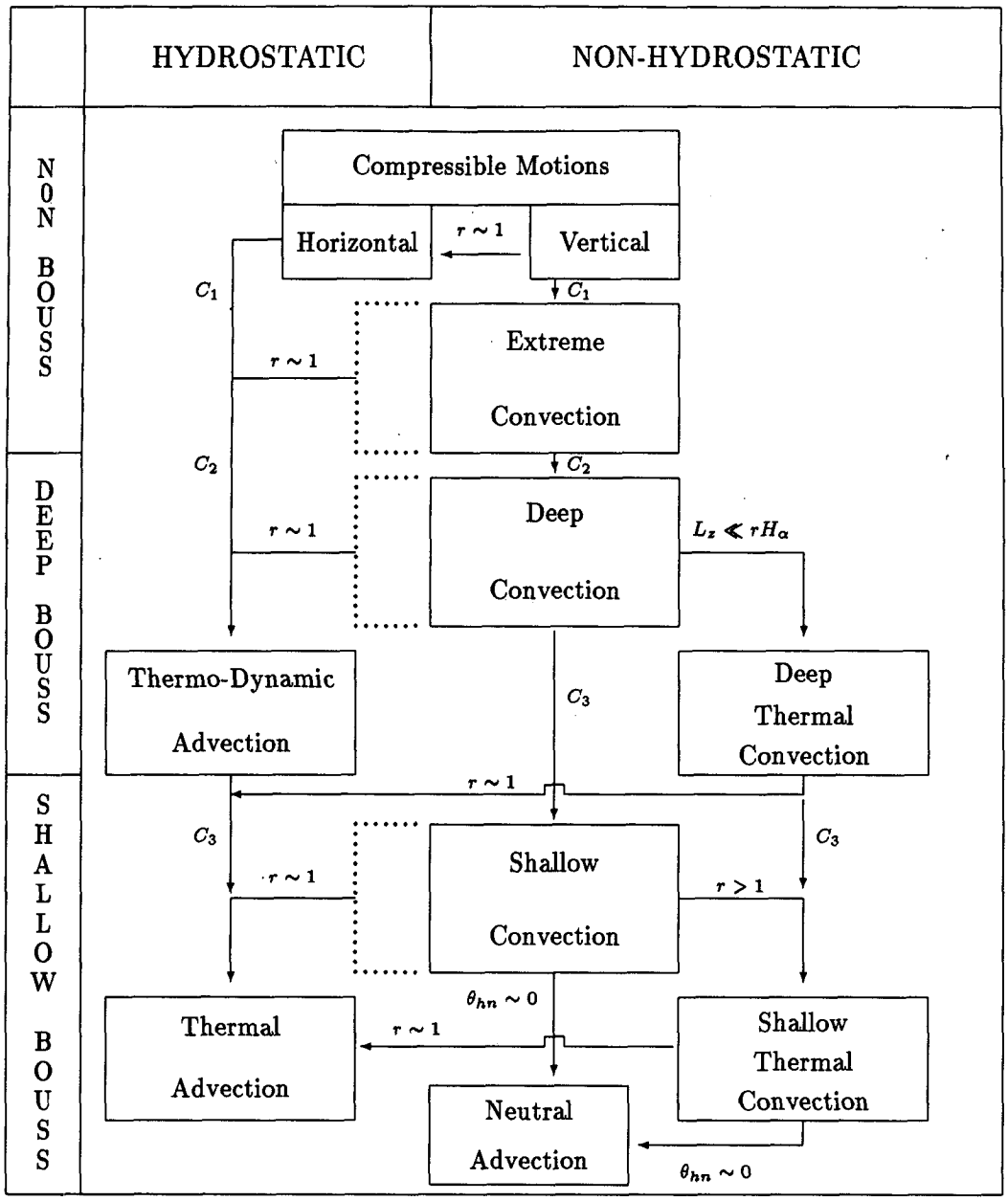

			Text Eqs.
CRITERIA	C_1	$\tau \gg \frac{\alpha_M}{\alpha_s}\left[\frac{L_H}{V_H}, \frac{L_z}{W}, \frac{H_\alpha}{W}\right]_{min}$	(25)
	C_2	$\tau \gg \frac{\alpha_M}{\alpha_s}\left[\frac{L_H}{V_H}, \frac{L_z}{W}\right]_{min}$	(21)
		$\left\|\frac{\alpha_M}{\alpha_s}\right\| \ll 1\ ,\ \left\|\frac{\alpha'}{\alpha_s}\right\| \ll 1$	(12), (26)
		$\frac{L_z}{H_\alpha} \leq 1\ ,\ \frac{V_H}{W} \leq \frac{L_H}{L_z}$	(19), (17)
	C_3	$\frac{L_z}{H_\alpha} \ll 1$	(13)

FIG. 2. Flow subclass chart, whose organization is explained in text and whose symbols are defined in appendix B.

analysis will now be applied to Boussinesq flows (appendix A) to complete a comprehensive hierarchy of criteria for the classification of mesoscale atmospheric flows.

The shallow Boussinesq flow subdivisions of Mahrt are now extended to the deep Boussinesq flows (appendix A) of Dutton and Fichtl by use of the scale analysis of Pielke (1984), in which each term of the full anelastic continuity equation (20) is scaled by the static-state density vertical advection term (in the form $W\alpha_s/H_\alpha$), yielding

$$\frac{\alpha_M}{\alpha_s}\frac{V_H}{W}\frac{H_\alpha}{L_H} + \frac{\alpha_M}{\alpha_s}\frac{H_\alpha}{L_z} + 1 = \frac{V_H}{W}\frac{H_\alpha}{L_H} + \frac{H_\alpha}{L_z}. \quad (27)$$

With the use of (12), the heart of the Boussinesq assumption, the advection of perturbation density (first two terms) is dropped, which implies that the sum of the final two terms of (27) must be of order one. Mahrt (1986) has shown that the practical limitations associated with the further assumption that each of these two terms is likewise of order one is minimal; this latter assumption implies criteria (17) and (19), respectively. Note, for deep Boussinesq motions, timescale criterion (25) reduces to the shallow Boussinesq form (21) of Mahrt, as the final two terms are equivalent. Remultiplication of the remaining final three terms of (27) by scale factor $W\alpha_s/H_\alpha$ produces the Boussinesq anelastic continuity equation (18) in Table 2. A summary of the above three criteria to move from extreme convection to the currently discussed deep convection flows is given in box C2 in Fig. 2.

As α_{hn} was eliminated from the continuity equation for deep Boussinesq motions, it can be eliminated from the momentum equations, except in the buoyancy term. Use of (12) allows linearization of the ideal gas law as

$$\frac{p_{hn}}{p_0} \sim \frac{T_{hn}}{T_0} - \frac{\alpha_{hn}}{\alpha_0}, \quad (28)$$

which when introduced in the buoyancy term produces the vertical equation of motion for *deep convection* (appendix A and Table 2). Examples of such deep convection models (Table 3) include GESIMA (Eppel et al. 1992) and the model of Peltier and Clark (1979). A quasi-Boussinesq model in this group, RAMS (Tripoli and Cotton 1982), neglects α_{hn} in all terms, except buoyancy (consistent with the Boussinesq approximation) and the Eulerian time change term in the continuity equation (which avoids numerical solution of an elliptic pressure equation).

The Boussinesq deep convection equations are now simplified by generalization of the Mahrt shallow-flow-scale analysis to two deep convection subclasses: limited (in depth) nonhydrostatic deep flows (called *deep thermal convection*) and hydrostatic *thermodynamic advection*. Deep convection flows are nonhydrostatic when buoyancy does not balance the vertical pressure gradient force (VPGF). From the ideal gas law and isothermal atmosphere scale-height H_i ($=RT_s/g$), a ratio r is defined between the scaled perturbation buoyancy and the scaled perturbation VPGF:

$$r = \left|\frac{\alpha_M}{\alpha_s}\frac{L_z}{H_i}\frac{p_s}{p_M}\right|. \quad (29)$$

During noninversion conditions, $H_i < H_\alpha$, while during inversion conditions, $H_i > H_\alpha$. Dutton and Fichtl (1969), however, have shown that differences remain small in both cases, and thus $H_i \sim H_\alpha$ is assumed below.

For hydrostatic ($r \approx 1$) deep Boussinesq motions, mesoscale pressure perturbations must be retained in both the VPGF and buoyancy terms. Such motions must be mostly horizontal and, hence, advective. As such flows are deep (L_z large) and hydrostatic (L_H very large), they occur at the upper end of mesoscale, merging with the macro-γ scale. Such flows are driven by both dynamic and thermal instabilities and, thus, are called thermodynamic advection flows (appendix A and Table 2). Such phenomena could include mountain waves and synoptic fronts and cyclones (Table 3), but no reference to a thermodynamic advection model has been found in the literature.

Scale analysis of the other deep Boussinesq subcase, that is, unstable thermal convection, shows that the perturbation pressure in the buoyancy term may be neglected. To demonstrate this, (29) is rearranged as follows:

$$\left|\frac{p_M}{p_s}\right| = \left|\frac{L_z}{H_\alpha}\frac{1}{r}\frac{\alpha_M}{\alpha_s}\right|. \quad (30)$$

To neglect p_M/p_s, (30) shows it is necessary that

$$L_z \ll rH_\alpha. \quad (31)$$

For flow depths at the upper limit of deep Boussinesq, that is, with

$$L_z \sim H_\alpha, \quad (32)$$

mesoscale perturbation pressure in the buoyancy term can be neglected only if

$$r \gg 1. \quad (33)$$

Such a large r, however, should also force neglect of the VPGF in the vertical equation of motion, which would produce vertical accelerations from thermal buoyancy bounded only by advection. It is thus prudent to limit L_z to a value nearer the lower end of deep Boussinesq. Thus, r cannot be as large as in (33), but only $r > 1$. This hypothesis should be tested by use of a deep thermal convection model with and without the VPGF.

For such deep Boussinesq flows, mesoscale perturbation pressure can thus be ignored in the buoyancy term, and the resulting motions in Table 2 and Fig. 2 are hence called deep thermal convection (appendix

A). Note, (31) is the upper limit on L_z, while its lower limit is the upper limit (13) of shallow flows. Also note that (31) allows for deeper vertical circulation depth as flows become more nonhydrostatic.

As mesoscale perturbation pressure must be evaluated for the VPGF anyway in primitive equation models, this approximation might not frequently be used in such models. In vorticity-mode mesoscale models, however, as all reference to mesoscale perturbation pressure is eliminated, this is a useful approximation. Examples of deep thermal convection models (Table 3) include the primitive equation FITNAH model (Gross 1990) and the vorticity-mode TVMnh model (Thunis 1995).

e. Shallow Boussinesq flows

When a given flow satisfies criteria (12), (17), (21), (26), and

$$L_z \ll H_\alpha,$$

[this latter instead of (19)], the flow is shallow Boussinesq. For such *shallow convection* (appendix A) flows, the continuity equation is incompressible (Table 2 and Fig. 2), because the above criteria allows for the vertical advection of basic-state density (fourth term) to be eliminated from (8); this changes the (deep) Boussinesq anelastic form of the continuity equation into the (shallow Boussinesq) incompressible form (appendix A). Note that such incompressible flows exist in a compressible (by gravity) atmosphere.

The corresponding form of the vertical equation of motion in Table 2 (see also Fig. 2) is similar to that for deep convection flows, except that the vertical variation of ρ_0 has been neglected as a result of the one changed criteria. Shallow convection models (Table 3) include MERCURE (Buty et al. 1988).

The shallow convection equations can be simplified for hydrostatic ($r = 1$) flows. With (13) in (30), mesoscale perturbation pressure drops out of the buoyancy term for such flows, called *thermal advection* (appendix A) in Fig. 2. Thermal advection models (Table 3) include TVM/URBMET (Schayes et al. 1995).

The shallow convection equations may also be simplified for nonhydrostatic motions in which perturbation buoyancy dominates the VPGF ($r > 1$). In such flows, perturbation pressure again drops from the buoyancy term, leading to *shallow thermal convection* (appendix A, Fig. 2, and Table 2). With increasing flow depth, such flows merge with the above-described deep thermal convection, and are thus located near the shallow end of that latter class. Such models (Table 3) include the microscale model of Sievers and Zdunkowski (1986) and the mesoscale model of Svoboda and Steckl (1994).

Note, with thermally neutral stability, another possible shallow motion case exists in which the thermal buoyancy (by definition) is zero, producing equality between p_M/p_s and α_M/α_s in (28). As the circulation is shallow ($L_z \ll H_\alpha$), r must thus be much less than unity, which indicates that buoyancy can be eliminated from the vertical equation of motion for *neutral advective* flows (appendix A and Fig. 2), and thus the VPGF is balanced by advective processes (Table 2). Mahrt (1986) has, however, pointed out that the pressure perturbation term must be retained in the buoyancy flux in the turbulent kinetic energy (TKE) equation. While the resulting set of equations is often used by engineers to study flows around buildings, a need exists for quantitative evaluation of this term. In addition, Fast and Takle (1988) point out that for such nonhydrostatic flows, it is incorrect to use a hydrostatic thermal advection model to simulate neutral (e.g., high wind speed) shallow PBL flows (Fig. 1) over surface roughness discontinuities or hills (Table 3), for example, as was done in URBMET (Bornstein 1975).

Turbulent kinetic energy production by wind shear, buoyancy, and mixed shear/buoyancy effects, respectively, are parameterized as eddy friction terms. Such processes produce zero average vertical velocities and are thus not mesoscale (or microscale) convective flows. Such processes produce only subgrid microscale modifications of mesoscale flows via diffusion, and thus the correct names for these vertical mixing mechanisms could be *mechanically driven, buoyancy driven,* and *mixed diffusion,* respectively (appendix A). Note, *forced convection* is synonymous in the current nomenclature with advective flow interactions with topographic features.

In summary, the most important effect of the deep and shallow Boussinesq assumptions on the governing equations is to ignore all density spatial variations, except in the buoyancy term. Note that the particular form of the linearized ideal gas law appropriate for each Boussinesq flow type is contained within the corresponding buoyancy term in the vertical equation of motion, except for neutral advection flows for which buoyancy is eliminated. In that case, the ideal gas law is given by (28).

4. Thermal energy equation

Criteria derived in the above scale analysis are now applied to the thermal energy equation, required in any mesoscale model. The objective is to ensure consistency between the thermodynamic and dynamic equations for each flow class. Note that no scaling argument has been developed yet to justify elimination of certain terms. As these terms are never even mentioned in most models, the current analysis starts with the complete thermal energy equation and drops these terms at what appears (based on the scale analysis developed above) to be the correct level in the current flow hierarchy.

While the first law of thermodynamics is formulated in terms of temperature, it is convenient in mesometeorology to rewrite it in terms of potential temperature

θ, as the turbulent heat flux is zero during adiabatic conditions. With the Poisson equation, the first law can be written as

$$\frac{d\tilde{\theta}}{dt} = \frac{\tilde{\theta}}{c_p}\frac{d\tilde{S}}{dt}, \tag{34}$$

which after averaging becomes

$$\frac{\partial\theta}{\partial t} + \mathbf{V}\cdot\nabla\theta + \overline{\mathbf{V}\cdot\nabla\theta'} = \frac{\theta}{c_p}\frac{\partial S}{\partial t} + Et. \tag{35}$$

Reynolds-mean quantities are still unbarred for convenience, and the scalar turbulent-advective entropy term Et is given by

$$Et = \overline{\frac{\theta'}{c_p}\frac{\partial S'}{\partial t}} + \frac{\overline{(\theta+\theta')(\mathbf{V}+\mathbf{V}')\cdot\nabla(S+S')}}{c_p}, \tag{36}$$

which after expansion of its last term becomes

$$Et = \overline{\frac{\theta'}{c_p}\frac{\partial S'}{\partial t}} + \frac{1}{c_p}\left[\overline{\theta\mathbf{V}\cdot\nabla S} + \overline{\theta\mathbf{V}'\cdot\nabla S'} + \overline{\theta'\mathbf{V}\cdot\nabla S'} + \overline{\theta'\mathbf{V}\cdot\nabla S} + \overline{\theta'\mathbf{V}\cdot\nabla S'}\right]. \tag{37}$$

Note, this is believed to be the first time that the above term has been mentioned in an analysis of the thermal energy equation.

To expand the entropy time derivative in (35), the definition of mean entropy

$$S = c_p \ln\theta$$

(which does not involve flux terms) is combined with Poisson's equation to produce

$$S = c_p \ln T - R \ln p.$$

Taking the local time derivative yields

$$\frac{\partial S}{\partial t} = \frac{c_p}{T}\frac{\partial T}{\partial t} - \frac{R}{p}\frac{\partial p}{\partial t}, \tag{38}$$

which, when used in (35), produces

$$\frac{\partial\theta_{hn}}{\partial t} + \mathbf{V}\cdot\nabla\theta + \overline{\mathbf{V}\cdot\nabla\theta'} = \frac{\theta}{T}\left[\frac{\partial T_{hn}}{\partial t} - \frac{\alpha}{c_p}\frac{\partial p_{hn}}{\partial t}\right]_D + Et, \tag{39}$$

where zero-valued time derivative $(\ )_0$ components leave only time-varying $(\ )_{hn}$ components in time derivatives and where the bracketed term represents external diabatic forcing.

This compressible motion form of the thermodynamic energy equation (39) thus includes intractable (cannot be parameterized by normal closure techniques) turbulent entropy fluxes in Et, an intractable turbulent temperature flux term, and temperature and entropy advection terms that cannot be put in flux form without the addition of density containing correction terms (as flow is compressible).

For extreme convection flows, the turbulent temperature flux term $\overline{\mathbf{V}'\cdot\nabla\theta'}$ in (39) becomes tractable (as it and the temperature advection term can be written in flux form) via continuity equation (20), which yields

$$\frac{\partial\theta_{hn}}{\partial t} + \overline{\frac{1}{\tilde{\rho}}\nabla\cdot(\tilde{\rho}\mathbf{V}\theta)} + \overline{\frac{1}{\tilde{\rho}}\nabla\cdot\tilde{\rho}\mathbf{V}'\theta'} = \frac{\theta}{T}\left[\frac{\partial T_{hn}}{\partial t} - \frac{\alpha}{c_p}\frac{\partial p_{hn}}{\partial t}\right]_D + Et. \tag{40}$$

Overbars are required because Reynolds decomposition of the instantaneous density $\tilde{\rho}$ $(= \rho + \rho')$, and consistency with the extreme convection vertical momentum and continuity equations in Table 2, introduces now tractable (in theory, via parameterization) fourth-order temperature turbulent flux terms.

As turbulent and mesoscale density perturbations were neglected (relative to its mean quantity) in the Boussinesq continuity and momentum equations, these are now likewise neglected in the Boussinesq thermal energy equation; that is, $\tilde{\rho}$ becomes ρ_0 in (40). In addition, Et is now dropped, analogous to the elimination of **Mt** in the extreme convection momentum equation. Although this might seem arbitrary in the absence of a scaling argument, it is hoped that future research will be able to produce such an analysis.

For the resulting deep convection flow equation, decomposition of mean variables into static-state and mesoscale components, followed by application of the deep Boussinesq criteria (C_2 in Fig. 2) changes the equation (Table 2) to

$$\frac{\partial\theta_{hn}}{\partial t} + \frac{1}{\rho_0}\nabla\cdot(\rho_0\mathbf{V}\theta_{hn}) + w\frac{\partial\theta_0}{\partial z} + \frac{1}{\rho_0}\nabla\cdot(\rho_0\overline{V'\theta'}) = \frac{\theta_0}{T_0}\left[\frac{\partial T_{hn}}{\partial t} - \frac{\alpha_0 p_0}{c_p}\frac{\partial}{\partial t}\left(\frac{p_{hn}}{p_0}\right)\right]_D, \tag{41}$$

where the steady-state p_0 term is included within the time derivative for the scale argument contained in the following paragraph.

This deep convection equation can be simplified for its thermal convection subclass by application of (31), which allows neglect of the pressure correction term, producing

$$\frac{\partial\theta_{hn}}{\partial t} + \frac{1}{\rho_0}\nabla\cdot(\rho_0\mathbf{V}\theta_{hn}) + w\frac{\partial\theta_0}{\partial z} + \frac{1}{\rho_0}\nabla\cdot(\rho_0\overline{V'\theta'}) = \frac{\theta_0}{T_0}\left(\frac{\partial T_{hn}}{\partial t}\right)_D. \tag{42}$$

The shallow Boussinesq flow criteria must be applied to (41), and not to (42) (as the pressure term is again required), to produce (Table 2)

$$\frac{\partial \theta_{hn}}{\partial t} + \nabla\cdot(\mathbf{V}\theta_{hn}) + w\frac{\partial \theta_0}{\partial z} + \nabla\cdot(\overline{V'\theta'}) = \frac{\theta_0}{T_0}\left[\frac{\partial T_{hn}}{\partial t} - \frac{\alpha_a p_a}{c_p}\frac{\partial}{\partial t}\left(\frac{p_{hn}}{p_0}\right)\right]_D, \quad (43)$$

where α_a has replaced α_0, consistent with the Boussinesq approximation for shallow flows.

Note that most shallow Boussinesq models assume $\theta_0/T_0 \sim 1$, which produces a 3% error at a height of 1 km. The above shallow convection equation (Table 2) is valid for both of its nonneutral stability subcases (thermal advection and thermal convection). This form is used in most mesomodels but without regard to consistency with their dynamic equations.

The commonly made assumption that diabatic heating is due only to vertical net radiative divergence produces

$$\left(\frac{\partial T_{hn}}{\partial t}\right)_D = -\frac{\alpha}{c_p}\frac{\theta_0}{T_0}\frac{\partial Q}{\partial z}, \quad (44)$$

where α is α_0 and α_a for deep and shallow Boussinesq flows, respectively. Horizontal radiative flux divergence can, however, be comparable to vertical divergence with small nonhydrostatic horizontal grid spacings, in particular at the edges of polluted urban boundary layers. Note, all above versions of the energy equation are also valid for hydrostatic flow cases.

5. Flow classification

Separate graphical representations of the Boussinesq mesoscale flow subclasses during stable and unstable conditions were constructed from order of magnitude estimates of the various length scales and flow-class separation criteria (ignoring effects from condensation) described above. Note that while these values are (for convenience) representative of the earth atmosphere in its midlatitudes, they could be derived for other latitudes and/or for other planets by use of the criteria presented above.

Boundaries between unstable condition flow subclasses described above are defined in Fig. 3 by the following limits: zones of unrealized atmospheric flows, upper and lower limits on thermal convection, upper limit on the micro-β scale, hydrostatic–nonhydrostatic transition, and shallow–deep flow limit. All flow-class boundaries in this and the next figure represent best estimates consistent with scale arguments presented above. As each flow-class limit line really represents a transition zone, more precise limits and slopes could be developed via numerical model simulation of impacts resulting from the approximations discussed above.

For example on its vertical axis, a daytime PBL depth of 1 km was assumed for the boundary between shallow and deep Boussinesq, while the 10-km height assumed for the corresponding density scale-height H_α was also taken as the deep Boussinesq limit. The horizontal axis ranges over all currently defined mesoscale subclasses and the micro-β scale, whose vertical limit has been set equal to its 200-m horizontal limit (assuming mainly isotropic microscale motions). Note, the smallest large scale (macro-δ) is represented by horizontal and vertical extensions of the deep end of the meso-β scale.

The figure excludes flows with physically unreasonable combinations of L_H and L_z, for example, flows with L_H of 200 km and L_z of 200 m, or with L_H of 200 m and L_z of 10 km. The transition from hydrostatic to nonhydrostatic has an approximate slope of unity, as the scale analysis of Pielke (1984) indicated nonhydrostatic effects when L_z became greater than L_H. It has further been assumed that the smallest horizontal hydrostatic length scale is about 5 km at a height of 200 m, the horizontal size at which nonhydrostatic effects began in the vertical velocity field for island breeze simulations by Thunis (1995).

The hydrostatic–nonhydrostatic line, in combination with the deep–shallow flow line, produces four flow regions. Note first the transition from thermal advection to thermodynamic advection with increasing circulation depth for hydrostatic flows. Also note that part of deep convection is divided off by criteria (31) to produce deep thermal convection, while part of shallow convection is likewise divided off by criteria $r = 1$ to produce shallow thermal convection. Note, the $r = 1$ criteria denotes a transition between VPGF and buoyancy-dominated nonhydrostatic flows, and not a physical extension of the hydrostatic flow regime. Note also, the dashed horizontal line that denotes the internal division between the two thermal convection subclasses.

The corresponding stable atmosphere representation (Fig. 4) shows a lower-density scale height, a lower PBL depth, and an assumed factor of 2 reduction in the meso-β-scale upper limit. These first two changes result from the reduction of vertical motion magnitude in stable atmospheres, while the latter is a reasonable estimate of the known reduced horizontal extent of thermal circulations with such stability, for example, land versus sea-breeze circulations. Numerical simulations could help better define these limits. Note also that both exclusion zone limits have been moved, consistent with the larger horizontal to vertical length-scale ratios in stable flows.

While the microscale limit is unchanged, the hydrostatic–nonhydrostatic transition line is shifted toward smaller scales to reflect that circulations are more likely hydrostatic in stable conditions (Martin and Pielke 1983). Thermodynamic advection, thermal advection, and shallow convection still exist, but thermal convection flows (with $r > 1$) cannot exist in stable conditions. Vertical motions in stable condition deep convection flows are thus forced by the VPGF and/or advection but not by buoyancy. Thus, nighttime

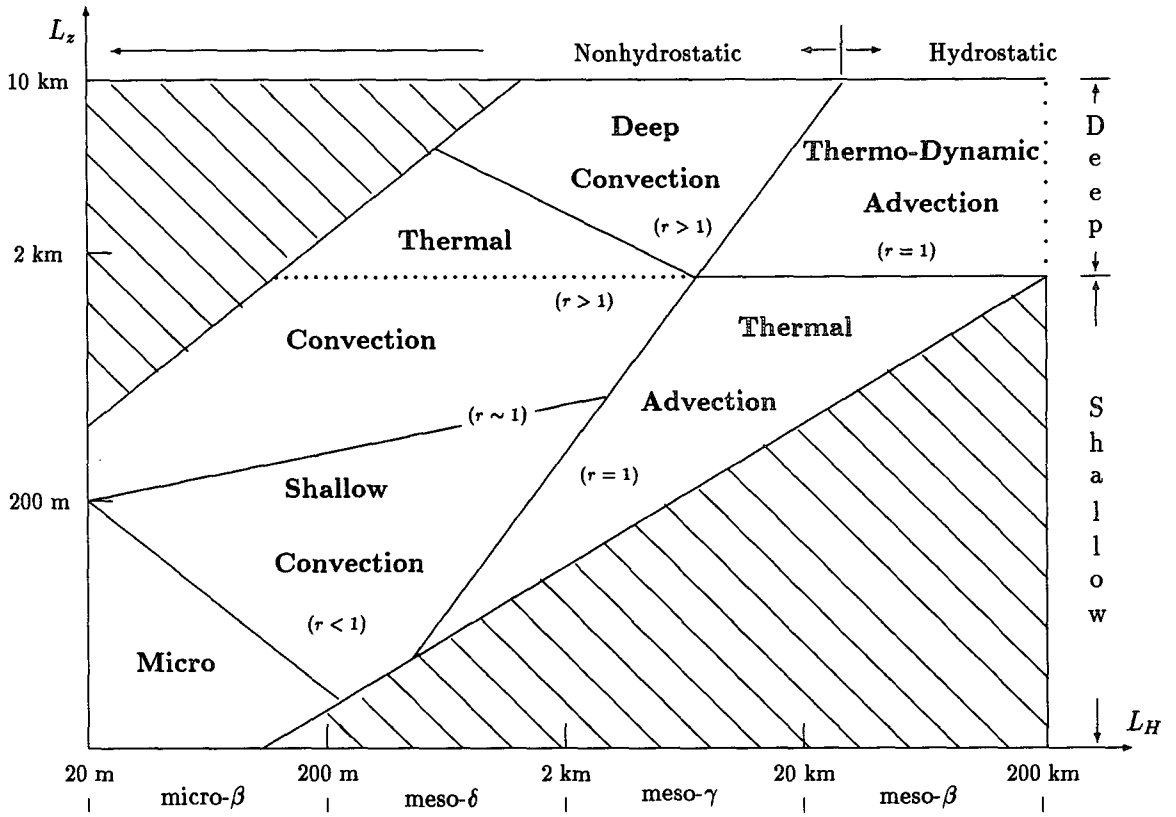

FIG. 3. Schematic of flow subclasses under unstable stability conditions, where hatched zones indicate nonphysical phenomena, dotted line indicates merging of thermodynamic advection with macroscale, r represents scaled ratio of buoyancy and VPGF perturbations, and dashed line represents division of thermal convection into its deep and shallow regimes.

convective motions have buoyancy acting as a restoring force and include gravity waves associated with mountain-induced flows, frontal lifting, and jet streaks.

Note, the equations of each subclass in Figs. 3 and 4 are less likely to accurately reproduce associated atmospheric phenomena as one moves upward and/or leftward within a subclass area.

6. Conclusions

This work could be considered as a response to the call by Hasse (1993) for a series of papers to stimulate discussion toward commonly accepted concepts in mesoscale meteorology. In that sense, its qualitative conclusions are open to discussion and consensus.

Different opinions exist concerning definitions of the time and space boundaries defining the micro-, meso-, and macrometeorological scales; Boussinesq approximations; anelastic equation of continuity; advection versus convection; and diffusion versus convection. The present research proposes a standard nomenclature (appendix A) and has integrated existing concepts of atmospheric space scales, flow assumptions, governing equations, and resulting motions into a hierarchy useful in the categorization of mesoscale models. Relationships between the hydrostatic and Boussinesq assumptions, relative to the proposed definitions of advective and convective flow types, are illustrated in Fig. 1.

In the proposed flow-class classification, the starting point was the complete (no approximations) set of mesoscale equations for non-Boussinesq flows. In the subsequent scale analysis, the deep and shallow Boussinesq flow divisions of Dutton and Fichtl were kept, as were the shallow flow subdivisions of Mahrt. In addition, the scale analysis approach of Mahrt was extended to deep Boussinesq motions. Limits of applicability of each derived flow-class equation set (with respect to atmospheric phenomena that can be simulated) were also discussed.

New dynamically based mesoscale time- and space-scale boundaries were proposed, consistent with the importance of the Coriolis force. Boundaries for each proposed macro-, meso-, and microscale subflow class are given in Table 1.

The proposed hierarchy of atmospheric motions is given in Fig. 2, which is organized into hydrostatic versus nonhydrostatic flow types, and then into non-Boussinesq, deep and shallow Boussinesq motions. The criteria used to differentiate each resulting flow class

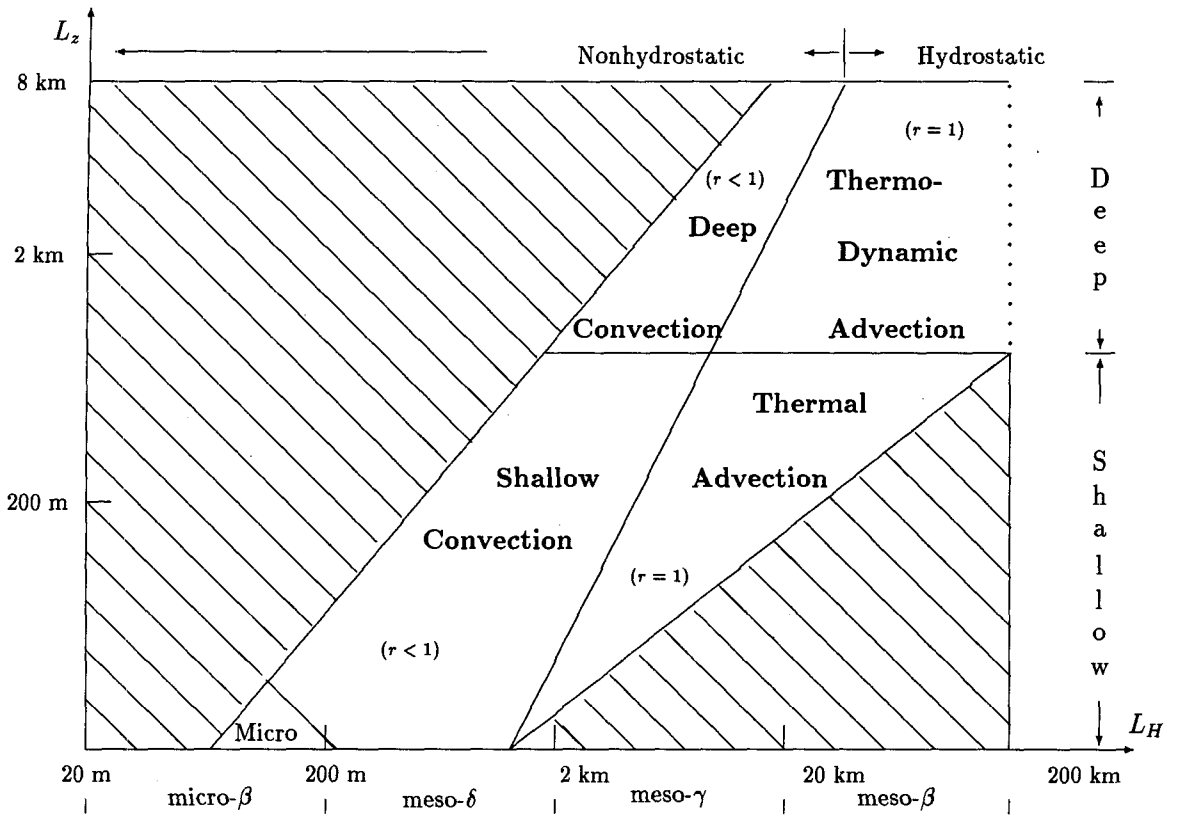

FIG. 4. As in Fig. 3 except for stable stability conditions.

(lower box of Figure) are discussed in the text, while the resulting corresponding governing thermodynamic and dynamic equations for each motion type are given in Table 2. Separate graphical representations during stable and unstable conditions (Figs. 3 and 4) of the spatial limits of each Boussinesq mesoscale flow subclass were constructed from order of magnitude estimates of the various proposed length scales and flow-class separation criteria. Note that while it is hoped that the proposed hierarchy contains all physically reasonable flow types, it does not include all theoretically possible combinations of assumptions, for example, hydrostatic extreme convection.

Certain phenomena, such as thunderstorms and mountain waves, have been simulated by a variety of equation sets that differ in their basic dynamic and thermodynamic assumptions. A summary of the consensus in the literature concerning the equation sets necessary to reproduce characteristics associated with specific atmospheric flow phenomena is given in Table 3, which also gives examples of models used to simulate many of the flow types in the table. Note, due to the difficulty of obtaining (from the literature) updated descriptions of equations used in current models, some references listed in the table could be updated.

Few studies have been carried out using simulation pairs (with and without a given assumption) to quantify the effects of a given assumption. For example, Schumann et al. (1987) simulated cumulus clouds using the nonhydrostatic compressible MESOSCOP model with and without a Boussinesq assumption. They found maximum changes of about 6% in computed velocities and about 20% in computed cloud particle concentration, although resulting fields did not exhibit significantly different structures. More such comparative studies are required to test the quantitative aspects of many of the ideas put forth in this paper.

As many model formulations are not completely described in the peer-reviewed literature, a volume containing such descriptions in a uniform format would be extremely useful for model comparison purposes. In addition, the design of a series of mesoscale modeling experiments that would involve application of a spectrum of model formulations would allow for evaluation of the limitations imposed by the modeling assumptions described above.

Acknowledgments. The authors would like to acknowledge helpful comments from Drs. H. Gallée, N.

Moussiopoulos, J. Walmsley, W. Thompson, R. Pielke, G. Schayes, and S. Cieslik.

APPENDIX A

Glossary of Concepts Developed in Text

Advection. Organized motions, in which horizontal velocity convergence (via mass continuity) produces vertical velocities at least an order of magnitude smaller. Subclasses include the following:

- *Thermal:* temperature-driven hydrostatic shallow Boussinesq advective flows.
- *Thermodynamic:* temperature- and pressure-driven hydrostatic deep Boussinesq advective flows.
- *Neutral:* nonhydrostatic advective flows under neutral static stability conditions.

Boussinesq flows. Motions in which (mesoscale and turbulent) perturbation density may be ignored, except in the buoyancy term where it is the linear sum of mesoscale pressure and temperature perturbations. Subclasses include the following:

- *Deep:* Boussinesq motions in which characteristic vertical length scale could be as large as characteristic density scale height; continuity equation is Boussinesq anelastic.
- *Shallow:* Boussinesq motions in which characteristic vertical length scale is much less than characteristic density scale height; continuity equation is incompressible.

Buoyancy term. Density–perturbation term in vertical equation of motion.

Compressible motions. Non-Boussinesq motions, in which Eulerian density time derivative is important in continuity equation. Subclasses include the following:

- *Vertical:* nonhydrostatic compressible motions.
- *Horizontal:* hydrostatic compressible motions.

Continuity equation. Forms include the following:

- *Compressible:* full equation.
- *Full anelastic:* temporal variation of density omitted.
- *Boussinesq anelastic:* temporal and spatial variations of density omitted, except for vertical static-state density variation.
- *Incompressible:* temporal and spatial variations of density omitted; flow is nondivergent.

Convection. Organized free (or thermal) or forced (or mechanical) nonhydrostatic motions, in which vertical velocities significantly impact horizontal velocities via mass continuity. Subclasses include the following:

- *Extreme:* non-Boussinesq convection.
- *Deep:* deep Boussinesq convection.
- *Deep thermal:* deep Boussinesq convection, in which perturbation density is function of temperature only and not pressure.
- *Shallow:* shallow Boussinesq convection.
- *Shallow thermal:* shallow Boussinesq convection, in which perturbation density is function of temperature only and not pressure.

Diffusion. Movement by microscale turbulent motions. Types include the following:

- *Buoyancy driven:* by temperature and/or pressure produced turbulence.
- *Mixed:* driven by wind shear and buoyancy produced turbulence.
- *Mechanically driven:* by wind-shear-produced turbulence.

Hydrostatic balance. Advective flows in which the VPGF and gravity are in near balance, although the difference between them must be larger than the sum of all other forces in the vertical equation of motion (Pielke 1984).

Reynolds.

- *Decomposition:* division of instantaneous variable into average and fluctuation components.
- *Assumption:* assumes spectral gap separation between resolvable scale (as defined in decomposition) and subgrid-scale motions. Existence of gap implies stationary, homogeneous resolvable mean flow. Allows use of ensemble averaging rules.

Scales of motion. Subscales include the following:

- *Macro:* organized hydrostatic tropospheric motions driven by dynamic instabilities and with a latitude-dependant Coriolis force.
- *Meso:* organized atmospheric motions with Coriolis force large enough to determine rotational direction but small enough to be assumed latitude independent; motions originate in troposphere.
- *Micro:* Nonhydrostatic motions with a Coriolis force too small to determine rotational direction.

Turbulence. Disorganized nonhydrostatic microscale fluctuations caused by buoyancy and/or mechanical shear processes.

APPENDIX B

List of Symbols

a. Roman

c_p	specific heat at constant pressure (=1005 J kg^{-1} K^{-1})
c_v	specific heat at constant volume (=718 J kg^{-1} K^{-1})
Et	scalar turbulent entropy terms
g	acceleration of gravity (=9.81 m s^{-2})
H_i	isothermal atmosphere scale height ($\approx$8 km)

H_α	density-scale height ($\approx$8 km)
L_H	scale horizontal circulation extent
L_z	scale circulation depth
Mt	vector turbulent momentum terms
p	atmospheric pressure
Q	radiative flux
r	buoyancy to VPGF ratio
R	gas constant (=287 J kg^{-1} K^{-1})
S	entropy
t	time
T	temperature
V	three-dimensional wind vector
V_H	scale horizontal speed
w	vertical wind speed component
W	scale vertical wind speed component
x, y, z	eastward, northward, and upward cartesian coordinate, respectively
CAT	clear-air turbulence
GCM	global circulation model
LLJ	low-level jet
PBL	planetary boundary layer
SBL	surface boundary layer
VPGF	vertical pressure gradient force

b. Greek

α	specific volume
δ	Kronecker delta
θ	potential temperature
μ	dynamic molecular viscosity
ρ	density
τ	scale time
ϕ	dummy variable
Ω	earth rotation vector

c. Subscripts

$(\ )_a$	volume average
$(\ )_D$	diabatic
$(\ )_h$	hydrostatic mesoscale perturbation
$(\ )_{hn}$	(nonhydrostatic plus hydrostatic) mesoscale perturbation
$(\ )_M$	mesoscale scale
$(\ )_n$	nonhydrostatic mesoscale perturbation
$(\ )_0$	static state
$(\ )_s$	synoptic scale

d. Special

$(\ )$	Reynolds decomposed average value (no over symbol)
$\overline{(\ )}$	Reynolds flux terms
$(\ )'$	turbulent perturbation
$\tilde{(\ )}$	instantaneous value
$\nabla(\ )$	three-dimensional del operator
$\nabla_H(\ )$	horizontal del operator
$\Delta(\ )$	difference operator

REFERENCES

Anthes, R. A., E. Y. Hsie, and Y. H. Kuo, 1987: Description of the Penn State/NCAR Mesoscale Model version 4 (MM4). NCAR Tech. Note NCAR/TN-282+STR, 66 pp.

Arya, P., 1988: *Introduction to Micrometeorology.* Academic Press, 307 pp.

Bartzis, J., A. Venetsanos, M. Varvayanni, N. Catsaros, and A. Megaritou, 1991: ADREA-I: A three-dimensional transient transport code for complex terrain and their applications. *Nucl. Technol.,* **94,** 135–148.

Bornstein, R. D., 1975: Two-dimensional URBMET urban boundary layer model. *J. Appl. Meteor.,* **14,** 1459–1477.

Boussinesq, J., 1903: *Théorie Analytique de Chaleur.* Vol. 2, Gauthier Villars.

Businger, J. A., 1982: Equations and concepts. *Atmospheric Turbulence and Air Pollution Modelling,* F. T. M. Nieuwstadt and H. van Dop, Eds., D. Reidel, 1–36.

Buty, D., J. Caneill, and B. Carissimo, 1988: Simulation numérique de la couche limite atmosphérique en terrain complexe au moyen d'un modèle mésométéorologique non-hydrostatique: Le code MERCURE. *J. Theor. Appl. Mech.,* **7,** 35–52.

Courtney, M., and I. Troen, 1990: Wind speed spectrum from one year of continuous 8 Hz measurements. Preprints, *Ninth Symp. on Turbulence and Diffusion,* Risø, Denmark, Amer. Meteor. Soc., 301–304.

Dudhia, J., 1993: A nonhydrostatic version of the Penn State–NCAR mesoscale model: Validation tests and simulation of an Atlantic cyclone and cold front. *Mon. Wea. Rev.,* **121,** 1493–1513.

Dutton, J. A., and G. H. Fichtl, 1969: Approximate equations of motion for gases and liquids. *J. Atmos. Sci.,* **26,** 241–254.

Eppel, D., D. Jacob, and H. Kapitza, 1992: Pollutant dispersion over the coastal zone of northern Germany. *Proc. Seminar on Monitoring and Modelling in the Mesoscale,* University of Thessaloniki, Greece, 117–134.

Fast, J. D., and S. Takle, 1988: Application of a quasi-nonhydrostatic parameterization for numerically modeling neutral flow over an isolated hill. *Bound.-Layer Meteor.,* **44,** 285–304.

Gallée, H., and G. Schayes, 1994: Development of a three-dimensional meso-γ primitive equation model: Katabatic winds simulation in the area of Terra Nova Bay, Antartica. *Mon. Wea. Rev.,* **122,** 671–685.

Gross, G., 1990: On the wind field in the Loisach valley—Numerical simulation and comparison with the LOWEX III data. *Meteor. Atmos. Phys.,* **42,** 231–247.

Hasse, L., 1993: Turbulence closure in boundary layer theory—An invitation to debate. *Bound.-Layer Meteor.,* **40,** 249–254.

Mahrt, L., 1986: On the shallow motion approximation. *J. Atmos. Sci.,* **43,** 1036–1044.

Martin, L. C., and R. A. Pielke, 1983: The adequacy of the hydrostatic assumption in sea breeze modeling over flat terrain. *J. Atmos. Sci.,* **40,** 1472–1481.

Moussiopoulos, N., T. Flassak, P. Sahm, and D. Berlowitz, 1993: Simulation of the wind field in Athens with the nonhydrostatic mesoscale model MEMO. *Environ. Software,* **8,** 29–42.

Oberbeck, A., 1888: On the phenomena of motion in the atmosphere. *Theory of Thermal Convection,* B. Saltzman, Ed., Dover, 162–183.

Ogura, Y., and N. W. Phillips, 1962: Scale analysis of deep and shallow convection in the atmosphere. *J. Atmos. Sci.,* **19,** 173–179.

Orlanski, I., 1975: A rational subdivision of scales for atmospheric processes. *Bull. Amer. Meteor. Soc.,* **56,** 529–530.

Peltier, W. R., and T. L. Clark, 1979: The evolution and stability of finite-amplitude mountain waves. Part II: Surface wave drag and severe downslope windstorms. *J. Atmos. Sci.,* **36,** 1498–1529.

Pielke, R., 1984: *Mesoscale Meteorological Modelling.* Academic Press, 468 pp.

Schayes, G., P. Thunis, and R. Bornstein, 1995: Development of the topographic vorticity mode mesoscale (TVM) model. Part I: Formulation. *J. Appl. Meteor.,* submitted.

Schumann, U., T. Hauf, H. Holler, H. Schmidt, and H. Volkert, 1987: A mesoscale model for the simulation of turbulence, clouds and flow over mountains: Formulation and validation examples. *Beitr. Phys. Atmos.,* **60,** 413–446.

Sievers, U., and W. G. Zdunkowski, 1986: A microscale urban climate model. *Beitr. Phys. Atmos.,* **59,** 13–40.

Spiegel, E. D., and G. Veronis, 1960: On the Boussinesq approximation for a compressible fluid. *Astrophys. J.,* **131,** 442–447.

Stull, R., 1988: *An Introduction to Boundary Layer Meteorology.* Kluwer Academic, 666 pp.

Svoboda, J., and J. Stekl, 1994: Mesoscale modelling of a flow modification caused by orography. *Meteor. Z.,* NF3, 233–241.

Thunis, P., 1995: Formulation and evaluation of a nonhydrostatic vorticity mode mesoscale model. Ph.D. dissertation, Université Louvain-la-Neuve, Catholique de Louvain, Belgium, 116 pp.

Tripoli, G. J., and W. R. Cotton, 1982: The Colorado State University three dimensional cloud/mesoscale model—1982 Part I: General theoretical framework and sensitivity experiments. *J. Rech. Atmos.,* **3,** 185–219.

Young, G. S., 1987: Mixed layer spectra from aircraft measurements. *J. Atmos. Sci.,* **44,** 1251–1256.